Virtual Colon Flattening

A. Vilanova Bartrolí[1], R. Wegenkittl[2], A. König[1], E. Gröller[1], and E. Sorantin[3]

[1] Institute of Computer Graphics and Algorithms
Vienna University of Technology
[2] Tiani Medgraph
[3] Section of Digital Information and Image Processing,
Department of Radiology, University Hospital Graz
Austria

Abstract. We present a new method to visualize virtual endoscopic views. We propose to flatten the organ by the direct projection of the surface onto a set of cylinders. Two sampling strategies are presented and the introduced distortions are studied. A non-photorealistic technique is presented to enhance the perception of the images. Finally, an approximate but real-time endoscopic fly-through is possible by using the data obtained by the projection technique.

1 Introduction

Virtual endoscopy deals with the inspection of hollow organs and anatomical cavities using medical imaging (e.g. CT and MRI) and computer visualization techniques. Virtual endoscopy has the potential of becoming a substitute of real endoscopy for some diagnostic procedures. A real endoscopy is invasive and, furthermore, involves a certain degree of risk for the patient.

Most of the virtual endoscopy techniques presented in the last years [1–3] concentrate on simulating the view of a real endoscope. This is the view that the endoscopists are used to. It can be useful for certain applications, like in an intraoperative scenario, but it is not necessarily the best way to inspect the inner surface of an organ. Actually, a real endoscope and organ are subject to physical limitations that a virtual endoscope and organ do not have. This paper considers virtual colonoscopy, which focuses on the examination of the colon. Physicians are mainly interested in visualizing the inner surface of the colon which is where polyps can be detected with endoscopy. It is important that the physician can estimate the size of polyps, since large polyps are more likely to develop into malignities. The usual endoscopic view visualizes just a small part of the surface. Furthermore, it is difficult to detect polyps that are situated behind the folds of the colon. An efficient way to inspect the inner surface would be to open and flatten the colon and then examine its internal surface. Unfortunately, this cannot be done in reality if we want that the patient survives. On the other hand, there is no patient damage if this dissection of the organ can be achieved virtually with the medical data obtained by CT or MRI (i.e. the virtual organ).

Some authors proposed a technique to straighten and unravel an organ virtually [4][5]. Their approach starts with defining a path which is placed as close to

the center of the object as possible. Then a sequence of frames is calculated. For each frame, a cross-section orthogonal to the path tangent is calculated. Then the central path is straightened and the cross-sections are piled to form a stack. As a last step the straightened colon is flattened obtaining a volume model of the flattened colon. The model is displayed afterwards using standard volume rendering techniques. This method allows to visualize the complete surface at once. One of the main problems of this technique appears in high curvature areas of the central path, i.e. at path locations where the radius of curvature is bigger than the organ diameter. In such cases orthogonal cross-sections intersect each other or are far apart in some other regions (see figure 1). As a consequence, a polyp can appear twice in the flattened model or it can be missed completely. Wang et al. in a later work [6] try to overcome this problem. They use electrical field lines generated by a locally charged path to govern curved cross-sections instead of the planar sections. The cross-sections tend to diverge avoiding conflicts, but the technique cannot ensure that they will not intersect. Haker et

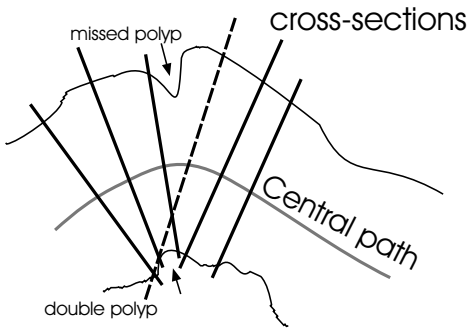

Fig. 1. Illustration of the possible undersampling and double counting of polyps due to intersections of the cross-sections in high curvature areas. The dash cross-section line produces a double counting of the polyp.

al. [7] use conformal mapping which is angle preserving to project the colon surface colored with the gaussian curvature to a plane. One of the main problems of this method is that a highly accurate segmentation is necessary to ensure good results in case they are used for diagnosis.

Paik et al. [8] propose other kinds of camera projections for virtual endoscopy. With a normal endoscopic view just 8% of the solid angle of the camera is seen in each frame. Paik et al. project the whole solid angle of the camera by map projection techniques used to map the world globe in charts. They suggest the use of the Mercator projection to map the solid angle to the final image. This technique samples the solid angle of the camera, then the solid angle is mapped onto a cylinder which is mapped finally to the image.

All of these methods introduce some kind of deformation since it is mathematically impossible to perform a mapping between two surfaces preserving

angles and area at the same time if the two surfaces do not have the same gaussian curvature.

In section 2, we propose a method to flatten the colon using a new camera projection technique. Section 3 presents different sampling options that cause different deformation problems. A minimization of the rotation for the camera movement is described in section 4. Section 5 describes a non-photorealistic technique that enhances the perception of the image. Then it is presented how an approximate but fast endoscopic view can be generated with the data calculated for the projection method. Finally, some results and studies with colon data are presented.

2 Method Overview

The methods proposed by Wang et al. [6] generate a flat model of the colon that later on will be carefully inspected by the physician. Our method will not generate a flat model of the whole colon, but allows to inspect locally flattened regions such that double counting of polyps does not occur.

The presented method involves moving a camera along the central path of the colon. The central path can be calculated using one of the common techniques used to skeletonize an object. We used a thinning algorithm which ensures topological preservation of the object (see Vilanova et al. [3]). The path is smoothed and finally approximated by a B-spline curve.

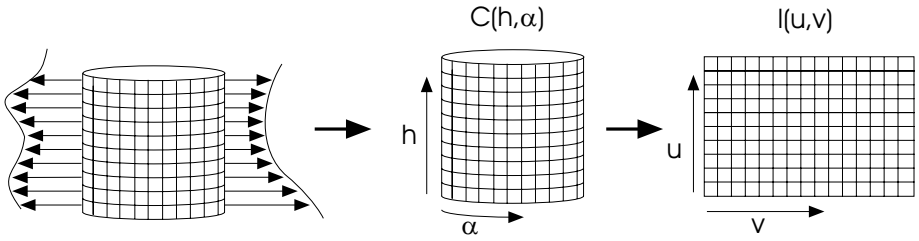

Fig. 2. Illustration of the projection procedure. A region of the surface is projected to the cylinder $C(h, \alpha)$. Then the cylinder is mapped to the image $I(u, v)$

For each camera position a small cylinder tangent to the path is defined. The middle point of the cylinder axis corresponds to the camera position. The length of the cylinder axis has a constant value for all camera positions. The length is defined by inspecting the camera path, and calculating the distance following the tangent between the path position and the colon surface. The length is defined by the distance that in any camera position ensures that the axis will not get out of the colon.

Rays starting at the cylinder axis and being orthogonal to the cylinder surface are traced (see figure 2). For each ray, direct volume rendering compositing is used to calculate the color which corresponds to the cylinder point where the

ray was projected. Finally, the colored cylinder with the sampled rays is mapped to a 2D image. This is done by simply unfolding the cylinder.

The result is a video where each frame shows the projection of a small part of the inner surface of the organ onto the cylinder. If the camera is moved slowly enough the coherence between frames will be high and the observer will be able to follow the movement of the surface.

In high curvature areas also the problem which corresponds to the intersection of cross-sections (see figure 1) appears. In the presented method, possible double sampling of polyps emerges just between frames. However, it does not cause a double counting of polyps since the human brain is able to track the polyp movement due to the coherence between frames. Moving along the central path in such a high curvature area, a polyp might move up and down (due to double sampling) but is clearly identified as a single object.

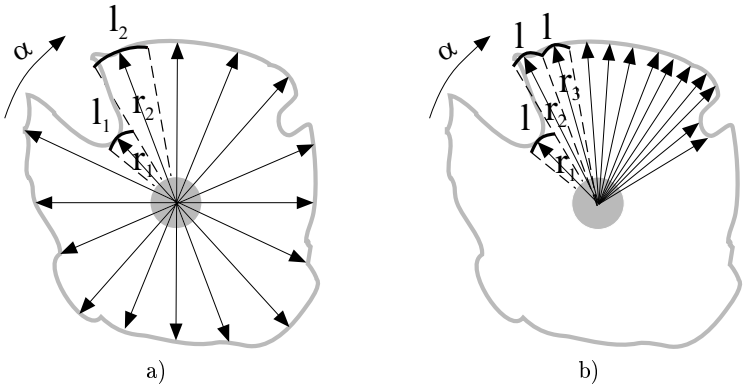

Fig. 3. a) Constant angle sampling: it is shown that different surface lengths are represented by the same length in the cylinder. **b)** Perimeter sampling: same length but different angle.

3 Projection onto a Cylinder

The proposed projection is illustrated in figure 2. A cylinder $C(h, \alpha)$ is defined for each camera position. This cylinder is colored by tracing rays orthogonal to the cylinder surface (i.e. projecting a region of the surface onto the cylinder). Then the cylinder is mapped to the final image $I(u, v)$ by a simple mapping function $f : (h, \alpha) \rightarrow (u, v)$.

The sampling distance (i.e. the distance between two consecutive rays) in the h-direction is constant, and it must be at most half of the size of a voxel (see figure 2). In this way the Nyquist frequency in the h-direction is preserved.

For each h-value the rays are traced in radial directions with respect to the cylinder axis. The rays are diverging from each other, so the volume data is not sampled uniformly if the incremental angle is constant (see figure 3a). In the

next section, two methods are described which project the organ surface onto the cylinder depending on the sampling of angle α : constant angle sampling and perimeter sampling.

3.1 Constant Angle Sampling

Constant angle sampling means that the angle between consecutive rays in α direction is constant for rays with the same h-value. Figure 3a illustrates how this sampling is done. Using this method, the cylinder is sampled uniformly but the surface itself is not uniformly sampled.

The advantage of this method is that the relation between both directions is locally preserved. Therefore the angles are locally preserved. An image generated by this method can be seen in figure 4a.

On the other hand, the area of the projected region is not preserved (see figure 3a). Therefore, the dimension of the projected polyps depends on the proximity of the cylinder axis and the diameter of the cavity. Consequently, the physicians cannot trust the sizes of the polyps.

Polyps can be missed with constant sampling (see figure 3a), if the angle increment is too large. If the sampling distance is too small the rays are traced where it would not be necessary. This makes the method inefficient.

3.2 Perimeter Sampling

In this section we propose a sampling strategy in which the rays are calculated so that the surface length that they represent is constant. A constant sample

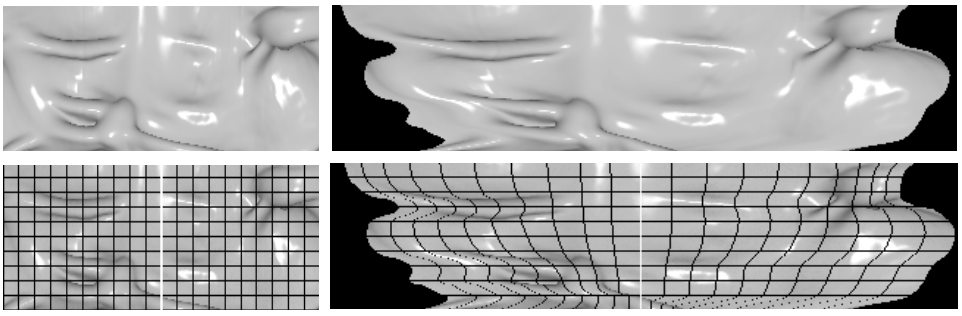

Fig. 4. a) Resulting image of the projection technique using constant angle sampling. **b)** Same camera position as a) but with a perimeter sampling. The bottom images show a grid which was generated by fixing a constant angle value.

length l is defined. l must be at most half the size of a voxel to keep the Nyquist frequency and therefore not to miss any important feature. l should have the same value as the sampling distance in the h-direction to preserve the ratio, or proportion, in the final mapping.

The algorithm incrementally calculates the ray directions which are in the plane defined by a certain value of h. The angle between the current ray and the next one is computed such that the length of the surface sample that the current ray represents is l in the α-direction (see figure 3b). The first ray is traced along an arbitrary angle α_0. α_0 must be the same for each value of h. r is defined as the distance from the cylinder axis to the surface point hit by the ray. The surface sample length in the α-direction that a ray represents is approximated by the arc with radius r. Therefore, the value of the angle increment for the next ray is estimated as $\frac{l}{r}$ radians.

This projection method projects the organ surface to a generalized cylinder whose radii are not constant within the cylinder. In this case the mapping function f maps uniformly the contours and also the surface of the generalized cylinder. Moving along the central path, contours of varying length are represented by varying numbers of rays. In the mapping to the image plane this results in the fact that in the v-direction (horizontal scanlines) typically only part of the pixels are covered by an unfolded contour. Therefore, the generalized cylinder is not mapped to the complete domain of the image (see figure 4b). The function f maps each sampled ray to a pixel in the image (i.e. each pixel corresponds to an area of $l \times l$ of the surface). The projected points that correspond to the rays at angle α_0 are positioned on a vertical line in the center of the image. Then from left to right the ray values are mapped to the image until the perimeter length is reached.

This projection has the area preservation property. So the relative sizes of surface elements are preserved in the image plane and do not depend on the proximity of the cylinder axis to the surface. On the other hand, a distortion is introduced with respect to the h and α-direction, so the angles are not preserved anymore. At the vertical center line of the image there is no distortion, but the distortion increases progressively when we move to the left and right. Figure 4b shows an image generated with perimeter sampling with a superposed grid which would correspond to a regular grid in a constant angle sampling of the cylinder. In this way, it can be observed how the horizontal lines are varying in extent according to the varying length of the corresponding contour.

4 Minimally Rotating Frame

In the previous section, a technique has been presented to project the surface of the organ onto the cylinder and then to the image.

At each position of the camera in the central path an orthogonal coordinate system is taken which specifies the location and orientation of the cylinder. One coordinate axis is given by the tangent vector of the central path. The other axes are in the plane orthogonal to the central path at the camera position. Taking the Frenet frame is not a good choice for this coordinate system. Firstly, the Frenet frame is not defined in linear portions of the central path. Secondly, by moving along the path the two vectors orthogonal to the tangent vector are rotating more than necessary, thus reducing coherence between adjacent frames. Therefore we investigate a rotation-minimizing coordinate frame.

We implemented the rotation-minimizing coordinate frame presented by Klok [9]. The coordinate frame is obtained by solving the following differential equation:

$$\begin{aligned} z(s) &= \frac{c'(s)}{\|c'(s)\|} \\ x'(s) &= -(c''(s) \cdot x(s))\frac{c'(s)}{\|c'(s)\|} \\ y'(s) &= -(c''(s) \cdot y(s))\frac{c'(s)}{\|c'(s)\|} \end{aligned} \tag{1}$$

where $c(s)$ represents the parametric central path and $(x(s), y(s), z(s))$ is the coordinate frame we are looking for. An initial orthogonal frame (x_0, y_0, z_0) is defined. Then the differential equations are solved using fourth order Runge-Kutta method. Theoretically, equations 1 produce orthogonal coordinate frames. To avoid accumulation of numerical errors (i.e. orthogonality is not ensured anymore), we take the following approach: $z(s)$ and $x'(s)$ are calculated according to the above formulas. Then $y(s)$ is taken as the cross-product of $z(s)$ and $x(s)$ $(y(s) = z(s) \times x(s))$. Finally we also correct $x(s)$ by taking it as the cross-product of $y(s)$ and $z(s)$ $(x(s) = y(s) \times z(s))$

5 Level Lines Enhancement

Using the distance of the hit surface point to the cylinder axis r, we can generate a depth image (see figure 6a). The depth image together with the shaded image represent a high field, similar to a landscape in topography. A good way to visualize landscapes in topographical maps is showing level lines, where each line correspond to a level of depth. The level lines improve the perception of depth and surface changes of the map.

The level lines are generated from the depth image. Firstly, the gradient of the depth image is calculated using a first derivative of the Gauss filter. The level lines are drawn based on the technique described by Saito et al. [10].

In order to improve the perception, a hue shift is applied to the level lines color. The colors of the lines are coded depending on the level of depth (see figure 6c). Hue shift has the advantage that it does not interfere with the highlights and dark areas of a shaded image. Technical illustration artists commonly use the temperature of colors in their drawing. The temperature of a color is defined as warm (red, orange and yellow) and cool (blue, violet and green). The temperature also gives depth cue information since the perception of the cool colors recedes whereas the perception of the warm colors advances. The hue shift has been chosen yellow-blue since these colors have a large shift range, and red-green is undesirable due to color blindness. Yellow corresponds to closer level lines and blue to level lines far away.

Once the level lines have been obtained they can be combined with the original shaded image (see figure 6d). The color of the shaded image should not be in the range between yellow and blue to achieve a good contrast. The level lines

provide information about the surface change and the distance of the surface to the cylinder axis.

6 Endoscopic View Generation

Once a polyp has been detected in the video of the flattened colon, the physician would be interested in seeing its location with an endoscopic view. Using the already calculated shaded images and depth images for each frame, a fast fly-through can be generated efficiently.

To generate the interactive navigation, the horizontal center lines of the depth images of the movie of the flattened colon are used. Knowing the camera location for each frame, the center lines can be backprojected to the 3D space (see figure 5a). A polygonal surface can be easily generated using triangle stripes. Each stripe corresponds to the triangles generated between one center line of the depth image and the center line of the next frame. We obtain a fast rendering since we use stripes and we render just the surface in the neighborhood of the camera (see figure 5). This can be achieved easily since the stripes are sorted by path position. With this method we achieve frame rates around 30f.p.s. with a Pentium II at 400 MHz with common OpenGL graphics hardware acceleration.

Each triangle can be colored by OpenGL with a correct lighting. Another option is to assign to each triangle vertex its color value calculated in the corresponding shaded image of the video of the flattened colon. The last option produces incorrect lighting but it has a better matching with the flattened colon images.

Obviously the resulting images are approximations and some artifacts appear due to the cross-section problem (see figure 1). However, it gives a good impression of the structure and it can be used by the physician to position the camera to the area that they want to visualize with a better quality but slower rendering.

7 Results

The images presented in this paper correspond to a CT data set of a cadaveric colon with a resolution of 381x120x632. The colon is 50 cm long and 13 artificial polyps were physically created in the cadaveric colon. These polyps had a size between 3.5x2.5 mm and 11.8x9.0 mm. Figure 6e shows an outside view of the segmented cadaveric colon and its central path together with the camera. The camera position corresponds to the image in figure 6g. Figure 6f is an endoscopic view moving the camera a bit backwards to show the same region as in figure 6g. It can be observed that the shape of the polyps is much more clear in the flattened images than in the endoscopic view figure 6f (please refer to http//www.cg.tuwien.ac.at/research/vis/vismed/ColonFlattening/) for the videos). The physicians who collaborate in this project could easily identify the polyps in the colon flattened images. Figures 4, 6b, 6d, 6g, and 6h show some of the polyps.

We also tested this method with a 256x256x311 CT data set of a colon. Figure 6i and 6j show the images generated from this data set. These figures were

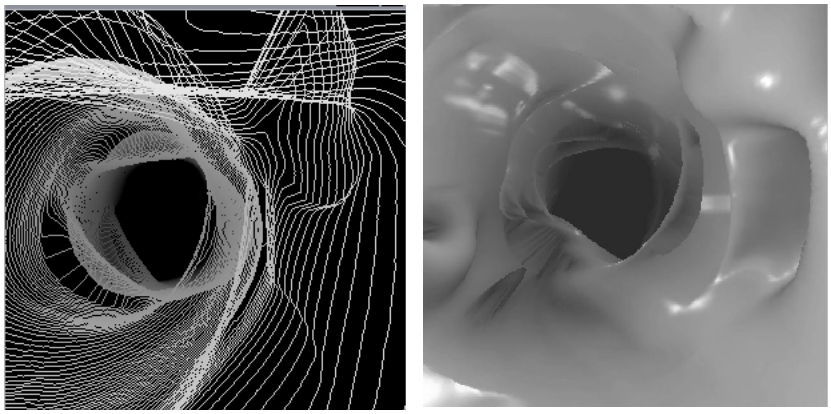

a) b)

Fig. 5. a) Endoscopic view backprojecting the lines using the depth information and the camera frame. **b)** Endoscopic view using the backprojection of the generated shaded stripes.

generated from the same camera position but the projection was done with constant sampling and perimeter sampling respectively. Both sampling techniques can be useful to the physician. Perimeter sampling preserves the area and allows the physician to evaluate the size of the polyps. While constant angle sampling preserves the angles and allows a better evaluation of the shape.

8 Conclusions and Future Work

We presented a new technique for virtual colonoscopy which does not simulate the usual endoscopic view. The images are generated with a projection technique that allows the physician to visualize most of the surface, and to easily recognize polyps that in an endoscopic view would be hidden by folds or would be hard to localize. The presented method avoids double counting of polyps. We presented two sampling strategies that respectively preserve the angle or area of the projected surface elements. We maximized the coherence between frames by minimizing the camera rotation. The images are also enhanced by calculating level lines which represent the depth. Finally we presented a technique to generate a real-time endoscopic view navigation by using the data of the video of the flattened colon.

As future work it is planned that the doctor is able to go back to the original data once the polyp has been detected. This can easily be done using the camera position of each frame of the video of the flattened colon.

It is also important that the cylinder axes do not get outside the organ. The cylinder height could be optimized for each data set and even adaptively defined depending on the camera position. The camera movement has to be specified in a way that we do not miss any surface region. In the current implementation, the

camera steps are so small that they ensure this, but the method is also inefficient because unnecessary images are calculated.

Another subject of future work is to extensively test the method with data of real patients with pathologies, to observe how the algorithm performs. The method might also be applied to other organs.

Acknowledgements

The work presented in this publication has been funded by the V^{is}M^{ed} project. V^{is}M^{ed} is supported by *Tiani Medgraph*, Vienna (`http://www.tiani.com`), and the *Forschungsförderungsfonds für die gewerbliche Wirtschaft*, Austria.
See `http://www.vismed.at/` for further information on this project.

We thank the Department of Radiology in Graz for their collaboration and for providing the data used in this paper. We thank Jiří Hladůvka for his collaboration concerning image processing techniques.

References

1. L. Hong, S. Muraki, A. Kaufman, D. Bartz, and T. He. Virtual voyage: Interactive navigation in the human colon. In *SIGGRAPH 97 Conference Proceedings*, Annual Conference series, pages 27–34. ACM SIGGRAPH, Addison Wesley, August 1997.
2. M. Wan, Q. Tang, A. Kaufman, Z. Liang, and M. Wax. Volume rendering based interactive navigation within the human colon. In *IEEE Visualization '99*, pages 397–400. IEEE, nov 1999.
3. A. Vilanova, A. König, and E. Gröller. VirEn: A virtual endoscopy system. *Machine GRAPHICS & VISION*, 8(3):469–487, 1999.
4. G. Wang and M.W. Vannier. GI tract unraveling by spiral CT. In *Proceedings SPIE.*, volume 2434, pages 307–315, 1995.
5. E. Sorantin, E. Balogh, K. Palagy, G. Werkgartner, E. Spuller, and S. Loncaric. *MEDICAL RADIOLOGY - Diagnostic Imaging*, chapter "Technique of Virtual Dissection of the Colon based on Spiral CT data". Springer Verlag Press, 2001.
6. G. Wang, S.B. Dave, B.P. Brown, Z. Zhang, E.G. McFarland, J.W. Haller, and M.W. Vannier. Colon unraveling based on electrical field: Recent progress and further work. In *Proceedings SPIE*, volume 3660, pages 125–132, May 1999.
7. S. Haker, S. Angenent, Allen Tannenbaum, and R. Kikinis. Nondistorting flattening maps and the 3d visualization of colon CT images. *IEEE Transactions on Biomedical Engineering*, 19(7):665–671, July 2000.
8. D.S. Paik, C.F. Beaulieu, R. B. Jeffrey, Jr. C.A. Karadi, and S. Napel. Visualization modes for CT colonography using cylindrical and planar map projections. *Journal of Computer Tomography*, 24(2):179–188, 2000.
9. F. Klok. Two moving coordinate frames for sweeping along a 3D trajectory. *Computer Aided Geometry Design*, 3:217–229, 1986.
10. Takafumi Saito and Tokiichiro Takahashi. Comprehensible rendering of 3-D shapes. In Forest Baskett, editor, *SIGGRAPH'90 Conference Proceedings*, Annual Conference Series, pages 197–206, August 1990.

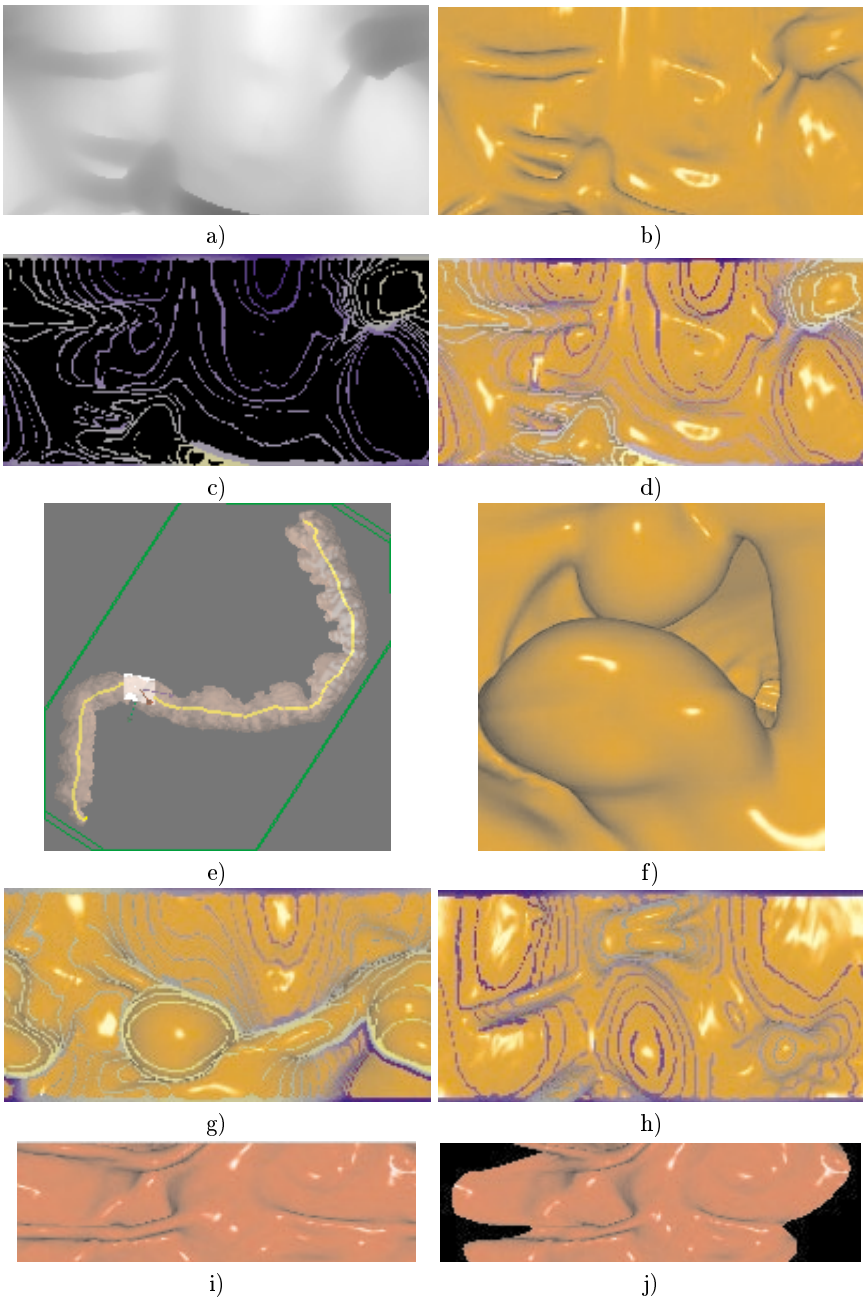

Fig. 6. Cadaveric colon CT data set 381x120x632. For the same camera position and using constant angle sampling: **a)** depth image **b)**shaded image **c)** level lines with hue shift color coded **d)** combination of the level lines and shaded image. **e)** Outside view and camera position for g). **f)** Endoscopy view moving the camera in e) a bit backwards. **g)** Constant angle sampling showing 2 polyps with level lines enhancement. **h)** Constant angle sampling from another camera positions showing 2 polyps.**Colon CT dataset 256x256x311**: **i)** Constant angle sampling. **j)** The same camera position as i) but with perimeter sampling.